Rheologica Acta Rheol Acta 25:296–307 (1986)

Slip flow of non-plasticized PVC compounds *)

W. Knappe and E. Krumböck

Institut für Kunststoffverarbeitung, Montanuniversität Leoben (Österreich)

Abstract: Measurements on seven rigid PVC compounds were carried out with a slit rheometer working in combination with an injection moulding machine. Plastication of the compounds occurred in the screw of the plastication unit, which also forced the melt through the die with a controlled forward velocity. The rectangular slit had a length of 90 mm and a width B of 20 mm. The height H could be varied between 0.8 and 3.3 mm. Pressures and temperatures were recorded at several positions in and before the die. Measurements were carried out at shear rates from 10 to 2000 s^{-1}.

When the reduced volume output $\dot{V}_{red} = \dot{V}/BH^2$ was plotted against the wall shear stress τ_W, only four compounds showed master curves independent of H, which is indicative of wall adhesion. In the other cases this plot did not produce such a master curve, but the plot of the mean velocity $\dot{V}/BH$ against τ_W was independent of H (slip curve). This indicated that slip flow prevailed with a slip velocity $v_G \approx \dot{V}/BH$.

When, in the case of wall slip, the smooth inner surfaces of the die were replaced by surfaces with grooves perpendicular to the direction of flow, slip flow was prevented and the flow curves $\dot{V} = f(\Delta p)$ were shifted to much higher values of Δp. Above a critical value of the wall shear stress (τ_{Wc}) at which slip flow began, the output became nearly independent of τ_W. From the measurements made below τ_{Wc} a τ vs. $\dot{\gamma}$ relation for the shear flow could be derived, which was used to calculate the superimposed shear flow $\dot{V}_S = f(\tau_W)$. Exact values of the slip velocity were then given by $v_G = (\dot{V} - \dot{V}_S)/BH$. Wall slip only occurred for compounds with a high shear viscosity, which corresponds to a high molecular weight (K-value).

Key words: Slip flow, PVC compound, injection moulding, grooved die surface, master curve

1. Introduction

The rheological behaviour of PVC compounds is strongly influenced by additives [1–3]. In the case of PVC compounds not containing plasticizers (rigid PVC) slip flow may occur due to the presence of lubricants or stabilizers acting as lubricants. Although this phenomenon is well known in the case of some polymer melts [4, 5], there has been little work on the slip flow of PVC and in particular on the quantitative dependence of the slip velocity on the wall shear stress, temperature, pressure etc.

Probably the first detailed investigation of slip flow for a rigid PVC compound was carried out by Offermann [6]. He used an emulsion-type PVC with a K-value of 70 and a high concentration (3%) of lubricant. The measurements were made with a capillary rheometer in combination with a single screw extruder with a bypass. Optical observations showed that slip flow could be prevented by small grooves in the die surface perpendicular to the direction of flow. In this case, the volume output $\dot{V}$ is given by the shear flow alone $\dot{V} = \dot{V}_S$. For a die of the same diameter but with a smooth surface one obtains a higher output for the same pressure gradient because of the superposition of slip ($\dot{V}_G$) on the shear flow. The slip velocity v_G may then be calculated by

$$v_G = (\dot{V} - \dot{V}_S)/A\,, \tag{1}$$

where $A = \pi D^2/4$ is the cross-section of the circular die. Offermann used the following equation to describe the dependence of v_G on the wall shear stress τ_W:

$$v_G = a_G \tau_W + b_G \tau_W^3\,, \tag{2}$$

where a_G and b_G are constants.

Chaffoureaux et al. [7] also employed grooved die surfaces to prevent slip flow. They used a slit rheometer in combination

*) Dedicated to Professor H. Janeschitz-Kriegl on the occasion of his 60th birthday.

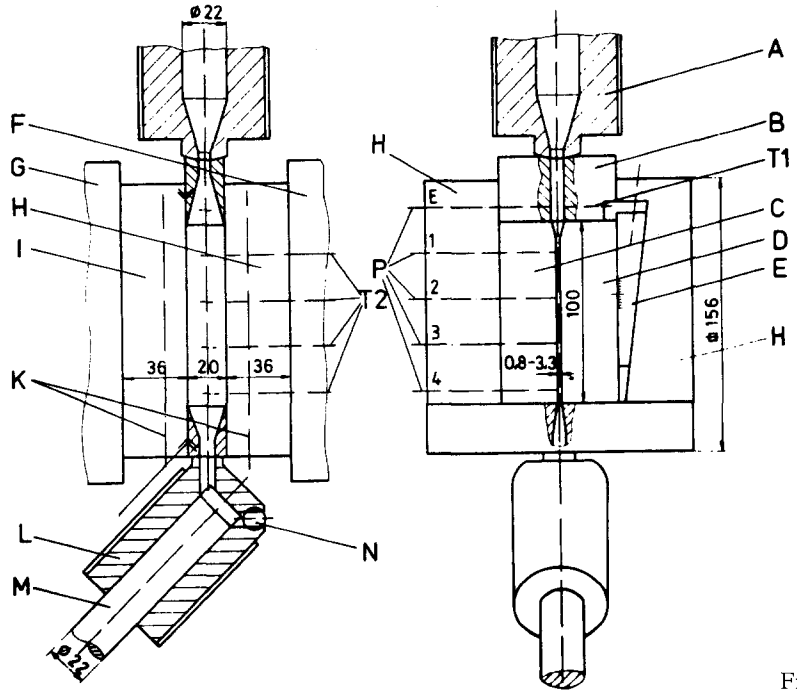

Fig. 1. Slit rheometer

with a single screw extruder. From measurements with a special Couette rheometer, they found a slip threshold at shear rates below 1 s^{-1}. Dies with grooved surfaces were also used in a recent study by Funatsu and Sato [8].

Here, we describe rheological measurements on seven rigid PVC compounds of practical importance in a range of shear rates from 10 to 2000 s^{-1}. The PVC compounds with low *K*-values showed wall-adhesion and those with higher *K*-values slip flow. Measurements were carried out with a slit rheometer in combination with a commercially available injection moulding machine. To prevent slip flow grooved dies were also used. The aim was to obtain data for calculating flow rates and pressure gradients that occur under the conditions of extrusion [1]).

2. Rheometer

The injection moulding machine (Engel ES 55/22) had a plasticating unit with a 22 mm diameter screw and a maximum shot volume of 27 cm^3. The maximum pressure exerted on the melt at the screw tip was 2000 bar. A metering screw with an L/D-ratio of 17 was used. The length of the metering section was 5 D and the channel depth was 1.75 mm. The maximum clamping force was 220 kN. The plastication unit was positioned vertically as shown in figure 1, and the clamping unit worked in the horizontal direction.

Figure 1 shows a cross-section of the rheometer. The nozzle of the plastication unit A was forced against the die inlet B. The two stainless steel blocks C and D formed a slit with a length of 90 mm and a width of 20 mm. The angle of the die inlet was 30°. The blocks C and D were held by the plates H and I, which could be kept at constant temperature by circulating oil through the bores K. The two plates of the clamping unit, F and G, forced together the plates H and I and the blocks C and D. After separating F and G the height of the slit could easily be set (with an accuracy of 0.02 mm) between 0.8 and 3.3 mm by displacing the wedge E.

Five pressure transducers (Dynisco and Staiger-Mohilo) were used to measure pressures and pressure gradients (denoted PE, P1, ..., P4 in figure 1). The error in the pressure measurements was always smaller than 10 bar. T1 was a probe used for measuring the melt temperature in the middle of the die inlet. Its tip pointed upstream into the flow [10]. Four thermocouples (T2) were placed near the die wall. In addition, the pressure transducers P2 and P3 were combined with thermo-couples. During the experiments the deviations from the mean temperature remained smaller than 1 K.

The calibration of the pressure transducers was carried out in the rheometer at a temperature of 160 °C. In this case block D was replaced by a calibration device covered with a special rubber membrane, which exerted a known hydraulic pressure on the transducers. This was done to avoid errors arising from dislocation of the transducers.

During the measurements the forward velocity of the non-rotating screw was held constant by the hydraulic control system of the injection moulding machine. The resulting volume output was measured by the displacement of the

[1]) A short description of the rheometer and some preliminary results with HDPE and two PVC compounds were presented at the IXth International Congress on Rheology in Acapulco [9].

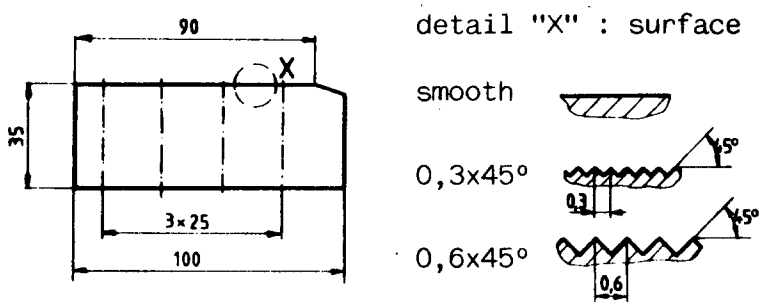

Fig. 2. Grooved die inserts

Table 1. Composition (by weight) of compounds showing wall adhesion

Material	Trade name	Compounds (parts per weight)			
		C1	C2	C3	C4
S-PVC, *K*-value 58	Solvic 258 RD	100	100	100	100
stabilizer	Irgastab 17 MOK	1.5	1.5	1.5	1.5
external lubricant	AC 316 A	0.2	0.2	0.6	0.6
internal lubricant	Radia 3200/4	1.0	2.0	1.0	2.0
colorant blue	U-blau 54	0.05	–	–	–
colorant red	PV-echtmarron FM01	–	0.05	–	–
colorant green	PV-echtgrün GG	–	–	0.05	–
colorant yellow	PV-echtgelb HR	–	–	–	0.05

piston M against a constant force, which could be varied by a hydraulic counter-pressure; approximately 60 bar was used. The electrically heated cylinder L could be emptied by opening the valve N.

The geometry of the die surface could be varied by changing the blocks C and D. Besides a smooth surface, two surfaces with geometrically similar grooves of different depths were chosen, see figure 2.

3. Materials

The granulated compounds were supplied by Halvic, Hallein (Austria). Table 1 lists the composition of the four compounds C1 to C4 in parts per weight. These compounds showed wall adhesion. They are typical of compounds used for the extrusion blowing of bottles, etc.

Table 2 lists the composition of the compounds C5, C6 and C7, which showed wall slip. Compounds of this kind are used in the extrusion of window frames and pipes. Compared to C6 and C7 the compound C5 had a greater concentration of fillers. All three of these compounds had higher *K*-values than C1 to C4.

The PVC compounds all had the same compounding history. Dry blends were produced with a fluid mixer from PVC powder and the additives. These blends were then extruded and granulated. This method of preparation is similar to that used in the IUPAC experiments on the rheological properties of rigid PVC [16]. Because a second plastication took place in the rotating screw of the injection moulding machine, it was expected that the melt would be homogeneous and no particle flow would occur. The homogeneity was evaluated by immersing the compound, which remained in the die after the experiment, in CH_2Cl_2 (the so-called "Methylenchlorid-Test" [17]). This gave similar results to the acetone test carried out in the work of den Otter et al. [18]. At a melt temperature of 190 °C none of the compounds showed any significant effects. However, at 175 °C the compound C6 showed strong deterioration as indicated by swelling and the occurrence of flakes.

4. Experiments

In preliminary experiments, the injection moulding machine was adjusted (in particular, the temperatures of the cylinder, the rotational speed of the screw and the plastication time) so that for a low volume output of 0.4 cm^3/s the melt temperature (at probe T1) was either 190 or 175 °C. In all cases a rotational speed of 35 min^{-1} and a plastication time of approximately 80 s

Table 2. Composition (by weight) of compounds showing wall slip

Material	Trade name	Compounds (parts per weight)		
		C5	C6	C7
E-PVC, *K*-value 72	Solvic 172 RB	50	50	–
S-PVC, *K*-value 64	Solvic 264 GA	50	50	–
S-PVC, *K*-value 68	Solvic 268 RC	–	–	100
stabilizer	Naftovin T 90	3.0	–	–
stabilizer	Austrostab 122	–	3.0	3.0
stabilizer (+ lubricant)	Austrostab 112	1.5	1.5	1.5
lubricant (+ stabilizer)	Austrostab 310	0.5	0.5	0.5
lubricant	Austrostab STS	0.3	–	–
lubricant	Loxiol G-21	–	0.2	0.2
chalk	Omyalite 95 T	10.0	–	–
chalk	Hydrocarb 90	–	4	4
pigment TiO_2	TLP 2	–	4	4
colorant brown	Sicopalbraun K 2795	2.0	–	–
colorant violet	PV-echtviolett RL spezial	–	0.1	–
colorant red	PV-echtrot B	–	–	0.1

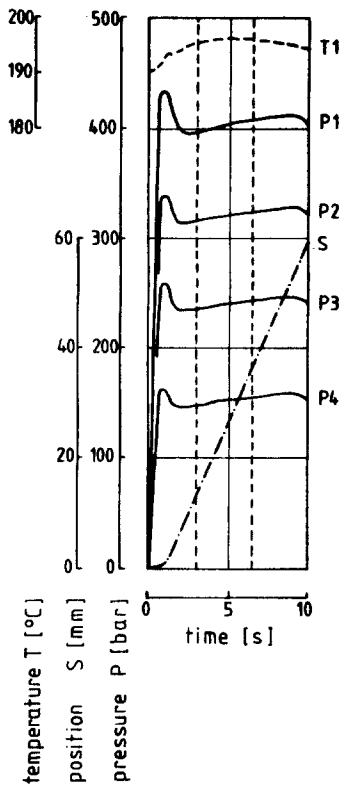

Fig. 3. Records of temperature, pressure and piston position during a measurement

were used; higher speeds led to an increase in melt temperature due to frictional heating. The use of constant temperatures provided a constant thermal history during plastication, which is comparable with the conditions in practical extrusion.

After the screw had reached its rear position (end of plastication), ninety seconds was allowed for the melt to reach thermal equilibrium. Then the melt was forced through the slit of the rheometer by the forward movement of the non-rotating screw with a constant velocity, which could be changed by setting a hydraulic valve. The volume outputs lay between 0.2 and 18 cm^3/s, corresponding to wall shear rates from 10 to 2000 s^{-1}.

During flow through the rheometer the temperature T1, the pressures P1, P2, P3 and P4 and the position S of the piston M (see figure 1) were recorded. Figure 3 shows an example of such a record. The maximum (or overshoot) in all pressure traces, which may be attributed to adiabatic compression and non-stationary effects at the beginning of the flow, is followed by a slow rise in the pressure, probably caused by friction in the cylinder L. Towards the end of the cycle, when the screw reaches its final position, the forward velocity and therefore the output and pressure decrease. The magnitude of the overshoot was found to increase with increasing output.

Except for some cases with high outputs and short test times, there was usually a constant pressure gradient between the transducers P1 and P4. For the rheological calculations, only the middle portion of the plots was used (i.e. for piston positions between 13 and 36 mm indicated by the dashed vertical lines in figure 3). In this region there was a slight rise in temperature. Griffith numbers were between 0.1 and 13, indicating that deviations from isothermal flow were significant. Despite this, no significant deviations from a linear decrease in pressure over the slit length were found. The melt temperatures were not corrected and

the quoted values were these prevailing with an output of 0.4 cm^3/s. For more details of the errors in measuring melt temperatures see [11].

5. Calculations

The pressure drop ΔP (= P1−P4) was measured for various outputs $\dot{V}$ and slit heights H. A reduced volume output was defined as

$$\dot{V}_{red} = \dot{V}/BH^2 = f(\tau_W)\,, \tag{3}$$

where B is the width of the rheometer slit. The wall shear stress was calculated by

$$\tau_W = \Delta P H/2L\,, \tag{4}$$

with L equal to 75 mm the distance between the pressure transducers P1 and P4 (see figure 1). The data were then plotted as $\dot{V}_{red}$ versus τ_W. If a single master curve was obtained, this indicated that wall adhesion was present for all experimental conditions.

A computer program was used to approximate the points of the master curve by the following functions:

1) Prandtl-Eyring formula (PRA-EYR)

$$\dot{\gamma} = C \sinh(\tau/A)\,, \tag{5}$$

where $\dot{\gamma}$ is the shear rate and A, $C > 0$ are constants.

2) Ostwald-de Waele formula (OST-WAE and OST-VAR)

$$\dot{\gamma} = \varphi \tau^n\,, \tag{6}$$

where $\varphi > 0$ and $n > 1$ are constants.

3) Weissenberg-Rabinowitsch formula (WEI-RAB)

$$\dot{\gamma} = a\tau + b\tau^3\,, \tag{7}$$

where a and b are constants.

The best approximation was that having the smallest sum of squared deviations according to

$$\sum (Ab)^2 = \sum_{i=1}^{Z} (\dot{V}_{red,\,meas} - \dot{V}_{red,\,calc})^2 \rightarrow \min\,. \tag{8}$$

Here (Ab) are the differences between the measurements ($\dot{V}_{red,\,meas}$) and the values given by the approximation function ($\dot{V}_{red,\,calc}$) for a constant wall shear stress. Z is the number of measurements.

Two different approximation methods were used for eq. (6): OST-WAE and OST-VAR. In the case of OST-WAE the approximation was made in double-logarithmic coordinates, whereas for OST-VAR the best approximation was found by an iterative process, as also for eq. (3). More details are given in [11].

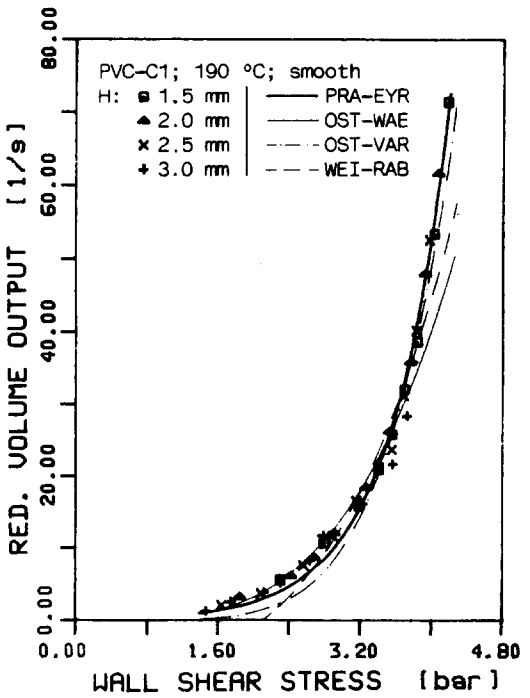

Fig. 4. Reduced flow curve $\dot{V}_{red}$ versus τ_W for C1

Figure 4 shows results for the compound C1. The experimental values give a master curve corresponding to wall adhesion. The calculations indicated that the Prandtl-Eyring formula (PRA-EYR) was the best approximation. This was also found in earlier work by Görmar [12].

If it is assumed that shear flow may be neglected (ideal plug flow), then the slip velocity is given by

$$v_G = \dot{V}/A\,. \tag{9}$$

In this case the flow curves obtained for various slit heights H also produce master curves (slip curves):

$$v_G = \dot{V}/(BH) = f(\tau_W)\,. \tag{10}$$

Since the measurements with compounds C5, C6 and C7 produced master curves when plotted in this form, it may be concluded that slip flow prevailed. Figure 5 shows such a slip curve for C6.

In the same way as for the reduced volume outputs, the data for C5 to C6 were approximated using the following functions:

1) SINH (analogous to the Prandtl-Eyring formula)

$$v_G = C_G \sinh(\tau_W/A_G) \tag{11}$$

with constants A_G and C_G;

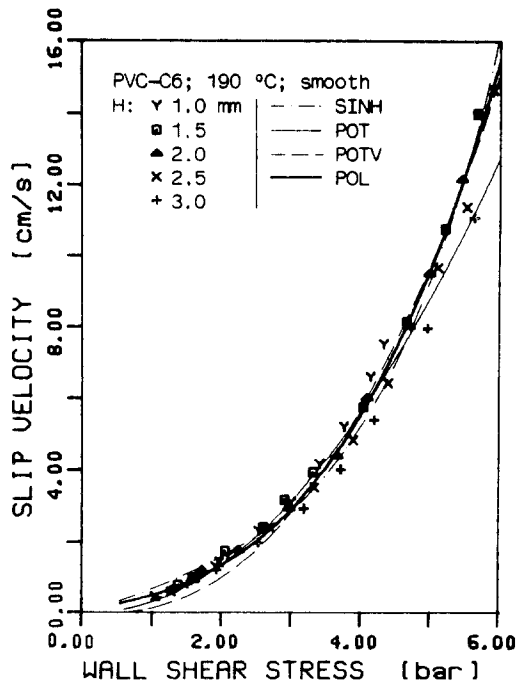

Fig. 5. Slip curve for C6

2) POT and POTV (analogous to the Ostwald-de Waele formula)

$$v_G = \varphi_G \tau_W^{n_G} \tag{12}$$

with constants φ_G and n_G;

3) POL (analogous to the Weissenberg-Rabinowitsch formula) with constants a_G and b_G, see eq. (2).

The best approximation was found by using eq. (8) with v_G substituted for $\dot{V}_{red}$. In case of eq. (12) the abbreviation POT denotes a linear regression in a double-logarithmic plot analogous to OST-WAE; POTV corresponds to OST-VAR. As can be seen from figure 5, the POL approximation using eq. (2) provides the best fit, in agreement with the results of Offermann [6], although SINH and POTV also fit the data quite well.

6. Results

The influence of additives on shear flow may be seen in figure 6, which shows the flow curves $\dot{V} = f(\Delta P)$ for the four compounds with wall adhesion (C1 to C4). Increasing the concentration of either lubricant shifted the flow curves to lower pressure gradients. With a rise in concentration from 1.2% (C1) to 2.6% (C4) the pres-

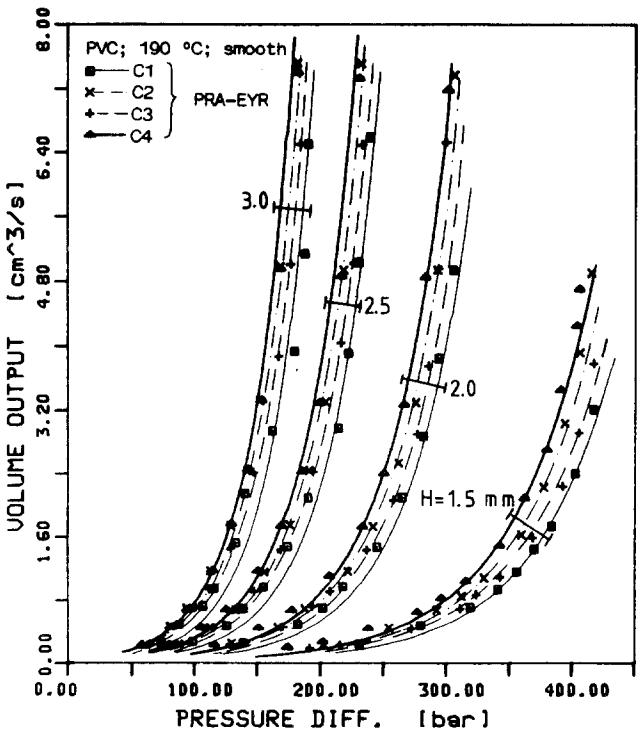

Fig. 6. Flow curves for C1, C2, C3 and C4 with various slit heights at 190 °C

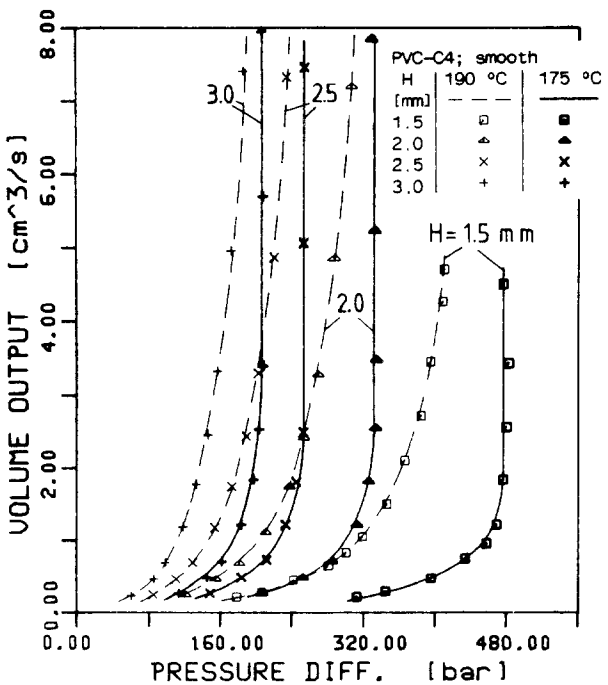

Fig. 7. Flow curves for C4 at melt temperatures of 175 and 190 °C

sure drop for a given output was lowered by just 8%. The curves in figure 6 were calculated from eq. (5). For all compounds, the value of the constant A was 0.58 bar ± 2%, whereas C rose with increasing lubricant concentration from 1.58 to 2.49 s^{-1}.

Some measurements were carried out with compound C4 at a melt temperature of 175 °C. Figure 7 compares the flow curves for the two temperatures and various slit heights H. At 175 °C there is a steep rise in output above a critical wall shear stress of about 4.3 bar, which can be attributed to the onset of slip flow. Above the critical value, the slip velocity seems to be independent of the wall shear stress. In addition, when wall slip occurred there was no significant deviation from linearity in pressure drop over the length of the slit.

Plotting the reduced volume output $\dot{V}_{red}$ against the wall shear stress in double logarithmic coordinates, one obtains figure 8. Above the critical wall shear stress the values measured at 175 °C do not lie on a master curve. There is also a shift of the critical wall shear stress to lower values with increasing H. In the range of wall adhesion both curves are similar and may be shifted vertically (τ = const) to give a master curve.

Table 3 shows the activation energies $E_{\dot{\gamma}}$ for various shear rates calculated according to the equation

$$\tau_{\dot{\gamma},T_1} = \tau_{\dot{\gamma},T_0} \exp\left[\frac{E_{\dot{\gamma}}}{R}\left(\frac{1}{T}-\frac{1}{T_0}\right)\right]. \qquad (13)$$

This table shows that the activation energies decrease with increasing shear rates. The values are near those for plasticized PVC [13, 14].

As mentioned above, figure 5 and eq. (10) show that the compounds with wall slip can be characterized by a slip curve if slip flow prevails. This is the case for the compounds C5, C6 and C7, whose flow curves are shown in figure 9. In spite of some remarkable differences in composition (see table 2), the flow curves are almost coincident for all three compounds.

Table 3. Activation energies of C4 at various shear rates

Range of temperatures [°C]: 175–190	
Shear rate [s^{-1}]	Activation energy [kJ/Mol]
50	48.0
100	43.5
150	41.9
200	41.2
250	40.1

Plotting the measured values as slip curves, the deviations from the master curve are less than 5%, see also figure 5. The best approximation for the slip curves is given by eq. (2) (POL). In figure 10 these curves are plotted for C5, C6 and C7, and the corresponding constants are listed in table 4.

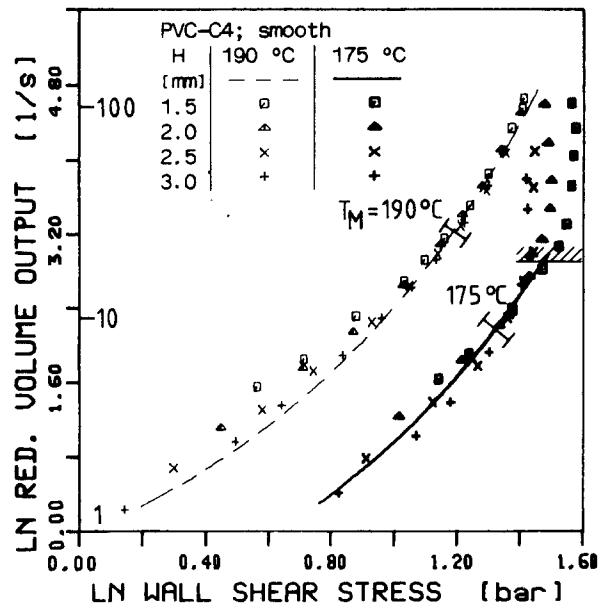

Fig. 8. Reduced flow curves for C4 at 175 and 190 °C

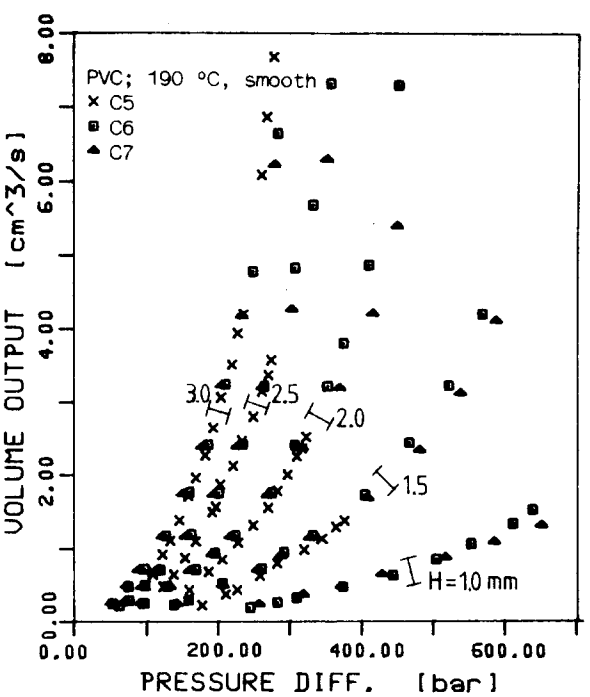

Fig. 9. Flow curves for C5, C6 and C7

Table 4. Constants in eq. (2) describing the slip curves for C5, C6 and C7 shown in figure 10; data analysed using eqs. (4) and (10)

Compound	Die surface	Melt temperature [°C]	φ_G $\left[\frac{cm}{s\,bar^{n_G}}\right]$	n_G [–]	a_G $\left[\frac{cm}{s\,bar}\right]$	b_G $\left[\frac{cm}{s\,bar^3}\right]$	τ_W [bar]
C5	smooth	190	0.187	2.30	(0.348)	(0.0569)*)	1.78–4.70
C6	smooth	190			0.427	0.0595	1.05–6.00
C7	smooth	190			0.612	0.0454	1.04–5.97
C6	smooth	175			0.0722	0.0400	1.86–6.70

*) In this case the POT approximation is slightly better than the POL approximation.

Table 5. Activation energies of C6 for various slip velocities

Range of temperatures [°C]: 175–190	
Slip velocity [cm/s]	Activation energy [kJ/Mol]
1	54.8
2	40.8
4	30.5
8	22.4
12	18.5

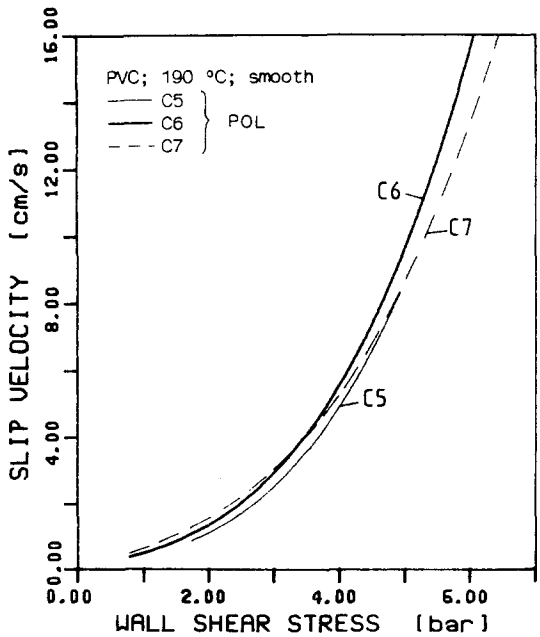

Fig. 10. Slip curves for C5, C6 and C7

In the case of C6 measurements were also carried out at a melt temperature of 175 °C. Both the slip curves for 190 and 175 °C are shown in figure 11. Instead of eq. (4), the following equation was used for calculating the wall shear stress:

$$\tau_W = \frac{\Delta P\, H B}{2L\,(B+H)}. \tag{14}$$

This resulted in a better master curve because in the case of plug flow the errors in calculating τ_W by the approximate eq. (4) are greater than for shear flow.

Analogous to eq. (13) an activation energy for slip velocity E_{v_G} can be calculated from the equation

$$\tau_{v_G, T_1} = \tau_{v_G, T_0} \exp\left[\frac{E_{v_G}}{R}\left(\frac{1}{T} - \frac{1}{T_0}\right)\right]. \tag{15}$$

Table 5 lists the activation energies calculated from the measurements shown in figure 11. There is a remarkable decrease in E_{v_G} with increasing slip velocity. Therefore the influence of temperature on slip velocity become smaller with increasing slip velocity. In the case of shear flow there is less influence of the shear rate on the activation energy of shear viscosity, see table 3.

The results described above were all obtained for smooth die surfaces. To evaluate shear flow in the case of prevailing wall slip, measurements were carried out with the grooved surfaces shown in figure 2. Flow curves for C4, a compound showing wall adhesion, with three die surfaces are shown in figure 12. In case of the grooved surfaces the slit height H is given as the distance between the tips. In all cases the grooved surfaces led to larger volume outputs than the smooth surfaces for equal pressure difference and equal values of H. Doubling the depth of the grooves produced only a small rise in output.

In figure 13 the reduced flow curves for the three different surfaces are given, approximated by eq. (5) (PRA-EYR). With increasing output the discrepancy between the curves increases. A fictive enlargement of H by a constant value ΔH in case of the grooved surfaces did not lead to coincidence of the curves.

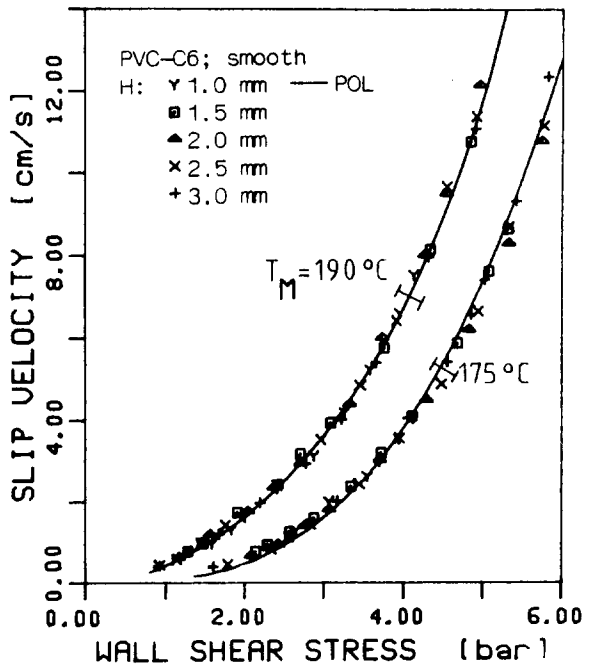

Fig. 11. Slip curves for C6 at melt temperatures of 175 and 190 °C

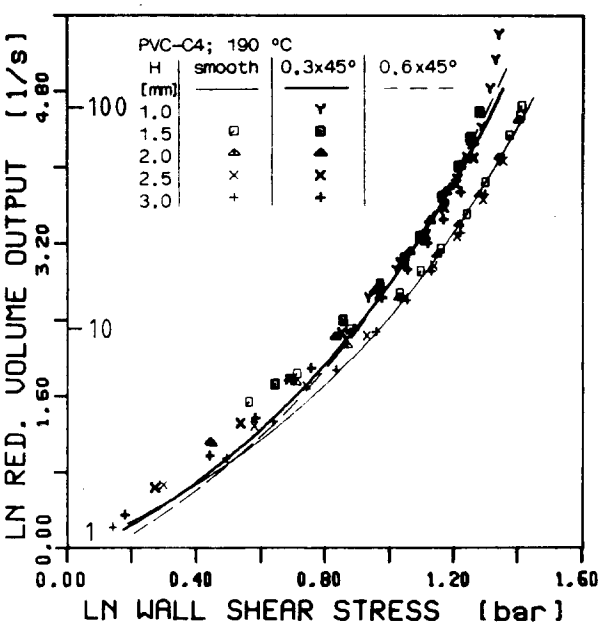

Fig. 13. Reduced flow curves for C4 with smooth and grooved die surfaces

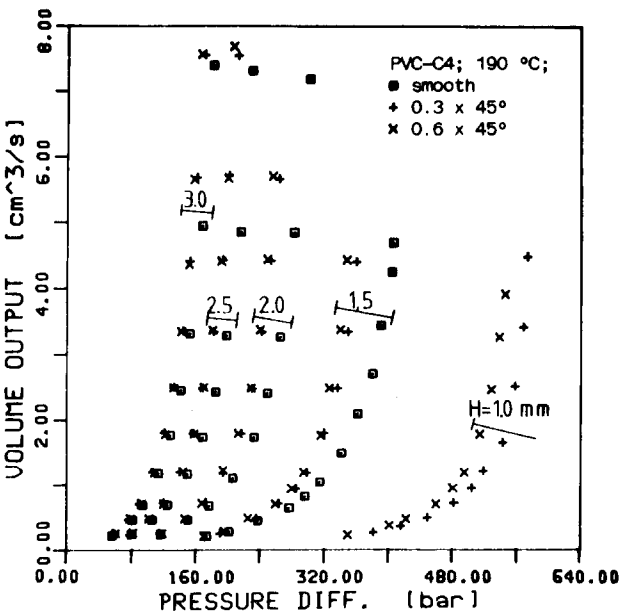

Fig. 12. Flow curves for C4 with smooth and grooved die surfaces

It is assumed that the transport of dissipated energy from the melt to the die wall is restricted by the melt in the grooves. Therefore the melt temperature near the grooved surface is higher than with a smooth surface, which leads to a lower viscosity near the surface and hence to an increase in output. Although this effect may be important, it cannot explain the small differences in the effects caused by grooves of different depth.

The prevention of slip flow by grooved surfaces was proven with two compounds that showed wall slip (C5 and C6). Figure 14 shows the flow curves for C5 with smooth and grooved die surfaces. It is seen that using grooved surfaces the flow curves are shifted to much higher pressure differences and end with a vertical slope, indicating wall slip. The two different groove geometries do not produce significant differences in the flow curves.

Figure 15 shows the reduced flow curves corresponding to figure 14. As expected, the flow curves obtained with smooth die surfaces and with wall slip do not coincide in figure 15. However, the flow curves with the grooved surfaces give a master curve, which can be well approximated by eq. (5) (PRA-EYR) up to a critical wall shear stress of about 5.5 bar.

Using this technique one can find the part of the shear flow that is superimposed on the slip flow. As figures 14 and 15 show, the fraction of volume output due to shear flow $\dot{V}_S/\dot{V}$ is small in relation to that due to slip flow and is about 10%. Therefore the slip curves in figures 5 and 10 are good approximations. The fraction due to shear flow becomes larger with increasing H.

If we compare the τ vs. $\dot{\gamma}$ relations for C_1 to C_4 with the τ vs. $\dot{\gamma}$ relations obtained for C_5 and C_6 by prevent-

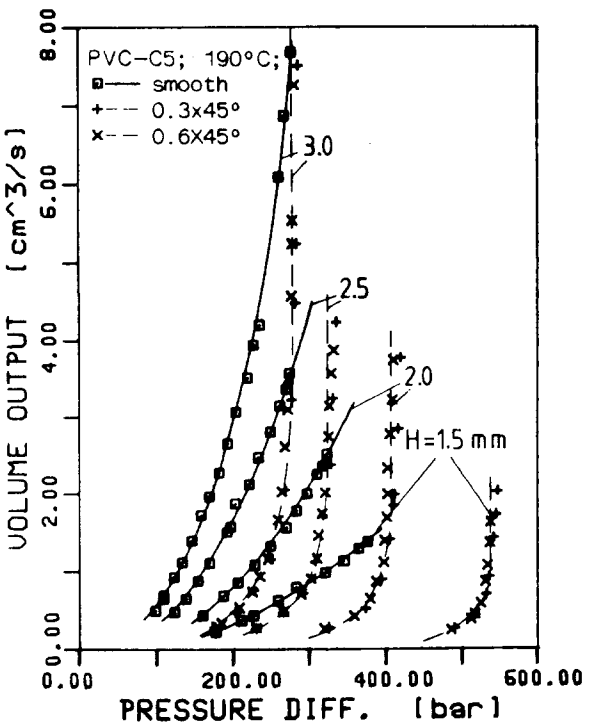

Fig. 14. Flow curves for C5 with smooth and grooved die surfaces

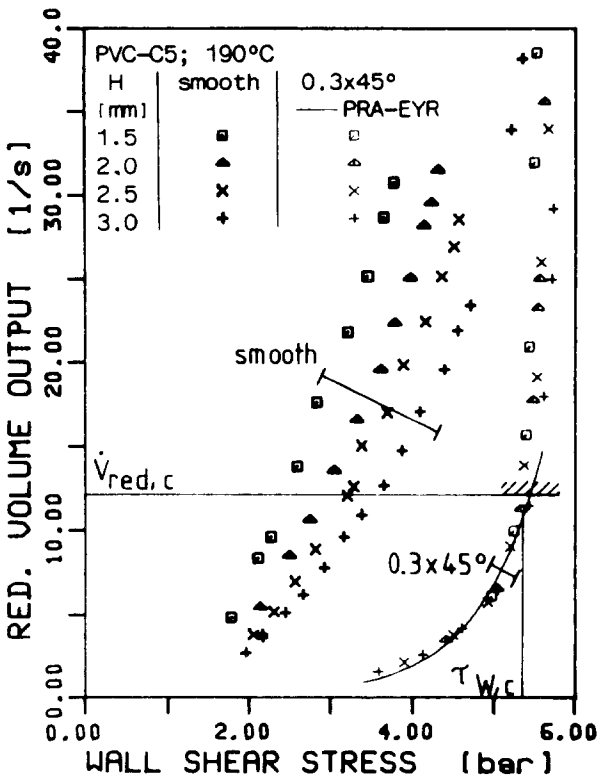

Fig. 15. Reduced flow curves for C5 with smooth and grooved die surfaces

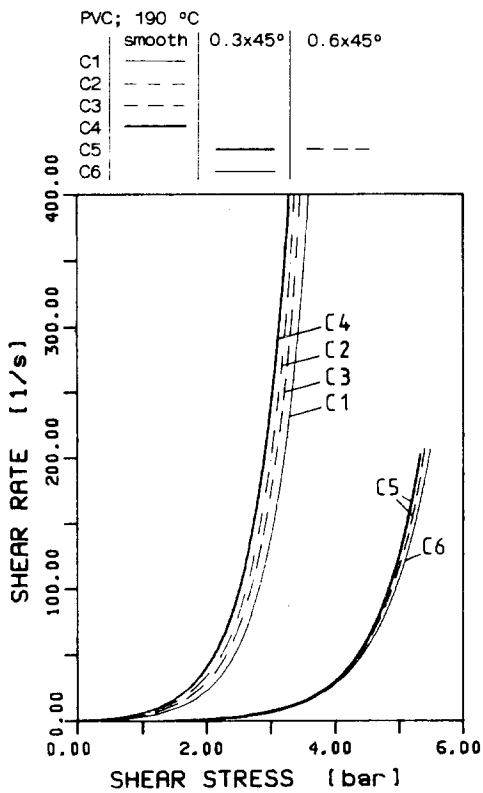

Fig. 16. τ vs. $\dot{\gamma}$ relations for PVC-compounds with and without wall adhesion

ing wall slip, we obtain figure 16. All the curves are approximations using the Prandtl-Eyring formula, eq. (5), which gave the best fit of the experimental results. The differences in the curves for C5 and C6 are within the limits of experimental error.

With these results we are able to correct the slip velocities found by assuming ideal plug flow, see figures 5 and 10. To a second approximation, slip velocities can now be calculated using eq. (1), since $\dot{V}_S$ may be derived from the τ vs. $\dot{\gamma}$ relation found with the grooved surfaces.

Since slip flow takes place only at the surface of the die wall, a much stronger influence of the wall temperature T_W should be expected than in the case of shear flow with wall adhesion. Measurements were carried out with a HDPE at a melt temperature T_M of 220 °C. With constant outputs, given by the forward velocity of the screw, we measured the dependence of the pressure differences ΔP on T_W, which could be changed by the temperature of the circulating oil. In figure 17, ΔP is plotted for constant T_M and constant output against the difference $T_W - T_M$. For HDPE with an output of 1.3 cm^3/s there was only a slight dependence of ΔP on $T_W - T_M$, as expected. With an

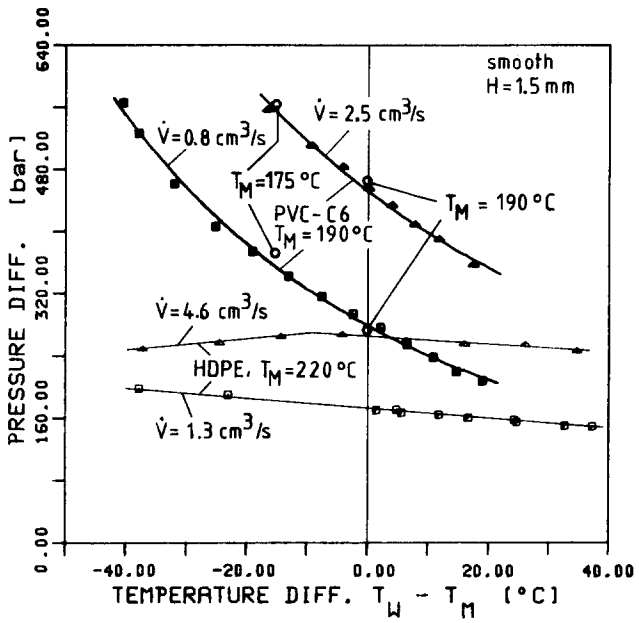

Fig. 17. Influence of wall temperature on the flow of HDPE and PVC-C6

output of 4.6 cm^3/s the influence of $T_W - T_M$ also remained small. It is possible that the change in slope at the left-hand side of the curve is caused by the greater dissipation of energy.

On the other hand, for the compound C6 a strong influence of the wall temperature is seen. Since slip flow prevails, the melt temperature should have little influence on ΔP and in fact ΔP should only depend on the temperature of the melt at the wall. Therefore the ΔP-value from the slip curve for 175 °C is nearly the same as ΔP measured with $T_M = 190$ °C and $T_W =$ 175 °C, see figure 17. Also the ΔP-values taken from the slip curve for $T_M = 190$ °C agree well with the plots of figure 17, which shows the good reproducibility of the measurements.

7. Discussion and conclusions

The combination of an injection moulding machine with a capillary rheometer had a number of advantages over a capillary rheometer used in combination with a single screw extruder with a bypass. For example, the thermal history of the plasticized compound did not change when the pressure drop or output was varied. Furthermore, a much greater range of pressures and outputs were obtained than is possible with a single screw extruder. The height of the slit could be quickly changed after opening the clamping unit. Therefore, the time and material requirements were smaller than for an extruder with a bypass. The advantages of a slit-rheometer have been described by Eswaran et al. [15]. The reproducibility of the pressure differences was such that the errors were smaller than 4%.

When the slip flow component of the flow is small, the method of Mooney [19] for evaluating the slip velocity leads to considerable errors, see [4, 6]. The master curves in this work corresponded to both extreme cases of the Mooney method: eq. (3) for $\dot{V}_G = 0$, and eq. (10) for $\dot{V}_S = 0$. In these cases one has the advantage that the results of all measurements, independent of H and τ_W, can be used for the master curve, which reduces the errors in the results. It was found that the slip velocities calculated by the Mooney method did not deviate more than 15% from the values derived from the master curves presented here.

The master curves for slip and shear flow and the corresponding equations can also be used for calculating pressure-output relations in extrusion dies by an iterative method.

On the basis of our experiments we cannot generally predict when slip flow will take place and when not. It seems that slip flow is favoured by a rather high shear viscosity, corresponding to high K-values. Our compounds C1 to C4 had K-values of 58, and slip flow was not observed at 190 °C. This agreed with the IUPAC-experiments [16], which showed that slip flow could be excluded for a K-value of 52 and temperatures higher than 180 °C. Offermann [6], on the other hand found slip flow with a K-value of 70. Further experiments are necessary with compounds having various K-values (molecular weight) but containing the same additives.

The slip effects cannot be explained by Coulomb friction as this would lead to an exponential decrease in pressure over the length of the slit [5], whereas in these experiments a linear decrease was always found. A possible explanation could be the presence of a thin layer of lubricant caused by flow-induced diffusion [20].

From the experimental results given here it can be seen that the energy dissipated during flow is not decisive for shear or slip flow. For a given power dissipation during flow either wall slip or wall adhesion is possible. However, for a given output, the power dissipated in a flow with wall slip was found to be lower than in a flow with wall adhesion. This was verified experimentally with grooved dies of equal dimensions [11].

Acknowledgements

We gratefully acknowledge the help of Halvic, Hallein (Austria) for supplying the compounds used in this work. For helpful discussions and remarks we are indebted to Professor K. Lederer.

References

1. Collins EA, Fahey TE, Hopfinger AJ (1982) Organic Coatings and Applied Polymer Science Proceedings 46:368–373
2. Collins EA (1977) Pure Appl Chem 49:581–595
3. Cernoch J, Stihel Z, Tluchor J (1980) Plaste u. Kautschuk 27:621–623; 28:200–202, 270–272
4. Berger R (1972) Plaste u. Kautschuk 19:113–118
5. Uhland E (1979) Rheol Acta 18:1–24
6. Offermann H (1972) Die Rheometrie wandgleitender Kunststoffschmelzen, untersucht am Beispiel von Hart-PVC. Dissertation TH Aachen
7. Chauffoureaux JC, Dehennau C, van Rijckevorsel J (1979) J Rheology 23:1–24
8. Funatsu K, Sato M (1984) Proceedings IX. Intl. Congress on Rheology. Mexico, vol 4 Applications, pp 465–472
9. Knappe W, Krumböck E (1984) Proceedings IX. Intl. Congress on Rheology. Mexico, vol 3 Polymers, pp 417–424
10. van Leuwen J (1967) Polym Eng Sci 7:1–12
11. Krumböck E (1984) Zum Wandgleiten von PVC-hart Mischungen im fließfähigen Zustand. Dissertation Montanuniversität Leoben
12. Görmar H (1968) Beitrag zur verarbeitungstechnischen Dimensionierung von Breitschlitzwerkzeugen für thermisch instabile Thermoplaste, insbesondere PVC-hart. Dissertation TH Aachen
13. Tse M (1981) Polym Eng Sci 21:1037–1045
14. Kuhn B (1977) Rheometrische Untersuchungen am System Polyvinylchlorid-Weichmacher. VDI-Verlag, Düsseldorf, Fortschritt-Berichte, Reihe 5, Nr 33
15. Eswaran R, Janeschitz-Kriegl H, Schijf J (1963) Rheol Acta 3:83–91
16. Wales JLS (1975) J Polym Sci, Symposium No 50: 469–485
17. Anonym: Kurzinformation: Methylenchlorid-Test. Deutsche Solvay-Werke GmbH, Solvic Kurzinformation 59, Ausg 1/73
18. den Otter JL, Schijf J, Wales JLS, Schwarzl FR (1974) Rheol Acta 13:209–215
19. Mooney M (1931) J Rheology 2:210–222
20. Janssen LPBM (1980) Rheol Acta 18:32–37

(Received March 11, 1985)

Authors' address:

Prof. Dr. W. Knappe
Institut für Kunststoffverarbeitung
Montanuniversität Leoben
A-8700 Leoben

Dr. E. Krumböck
Chemie Linz AG
A-4020 Linz